Plasmonic resonance of whispering gallery modes in an Au cylinder

Xining Zhang, Zhe Ma, Huakang Yu, Xin Guo, Yaoguang Ma, and Limin Tong *

State Key Laboratory of Modern Optical Instrumentation, Department of Optical Engineering, Zhejiang University, Hangzhou 310027, China
**phytong@zju.edu.cn*

Abstract: We demonstrate whispering gallery (WG) resonance of surface plasmon polaritons (SPPs) in a 2-dimensional confined Au cylinder by self interference. Despite the leakage of SPPs along the axis of the cylinder, Q factors of 375 are obtained in a cylinder with diameter of 30 μm. The coupling-angle-dependence of the WG resonance is also investigated. Our results open opportunities for a new category of plasmonic cavities with 2-dimensional confinement, and this may be applied to a variety of simple and natural metallic micro or nanostructures.

OCIS codes: (160.3900) Metals; (240.6680) Surface plasmons; (140.3945) Microcavities; (130.3990) Micro-optical devices.

References and links

1. W. L. Barnes, A. Dereux, and T. W. Ebbesen, "Surface plasmon subwavelength optics," Nature **424**(6950), 824–830 (2003).
2. B. Min, E. Ostby, V. Sorger, E. Ulin-Avila, L. Yang, X. Zhang, and K. Vahala, "High-Q surface-plasmon-polariton whispering-gallery microcavity," Nature **457**(7228), 455–458 (2009).
3. R. Perahia, T. P. M. Alegre, A. H. Safavi-Naeini, and O. Painter, "Surface-plasmon mode hybridization in subwavelength microdisk lasers," Appl. Phys. Lett. **95**(20), 201114 (2009).
4. M. Kuttge, F. J. García de Abajo, and A. Polman, "Ultrasmall mode volume plasmonic nanodisk resonators," Nano Lett. **10**(5), 1537–1541 (2010).
5. M. W. Kim, Y. H. Chen, J. Moore, Y. K. Wu, L. J. Guo, P. Bhattacharya, and P. C. Ku, "Subwavelength surface plasmon optical cavity—scaling, amplification, and coherence," IEEE J. Sel. Top. Quantum Electron. **15**(5), 1521–1528 (2009).
6. S. I. Bozhevolnyi, V. S. Volkov, E. Devaux, J. Y. Laluet, and T. W. Ebbesen, "Channel plasmon subwavelength waveguide components including interferometers and ring resonators," Nature **440**(7083), 508–511 (2006).
7. E. J. R. Vesseur, F. J. García de Abajo, and A. Polman, "Modal decomposition of surface-plasmon whispering gallery resonators," Nano Lett. **9**(9), 3147–3150 (2009).
8. X. Guo, M. Qiu, J. M. Bao, B. J. Wiley, Q. Yang, X. N. Zhang, Y. G. Ma, H. K. Yu, and L. M. Tong, "Direct coupling of plasmonic and photonic nanowires for hybrid nanophotonic components and circuits," Nano Lett. **9**(12), 4515–4519 (2009).
9. Y. F. Xiao, B. B. Li, X. Jiang, X. Y. Hu, Y. Li, and Q. H. Gong, "High quality factor, small mode volume, ring-type plasmonic microresonator on a silver chip," J. Phys. At. Mol. Opt. Phys. **43**(3), 035402 (2010).
10. H. Ditlbacher, A. Hohenau, D. Wagner, U. Kreibig, M. Rogers, F. Hofer, F. R. Aussenegg, and J. R. Krenn, "Silver nanowires as surface plasmon resonators," Phys. Rev. Lett. **95**(25), 257403 (2005).
11. H. T. Miyazaki, and Y. Kurokawa, "Squeezing visible light waves into a 3-nm-thick and 55-nm-long plasmon cavity," Phys. Rev. Lett. **96**(9), 097401 (2006).
12. J.-C. Weeber, A. Bouhelier, G. Colas des Francs, L. Markey, and A. Dereux, "Submicrometer in-plane integrated surface plasmon cavities," Nano Lett. **7**(5), 1352–1359 (2007).
13. M. Allione, V. V. Temnov, Y. Fedutik, U. Woggon, and M. V. Artemyev, "Surface Plasmon Mediated Interference Phenomena in Low-Q Silver Nanowire Cavities," Nano Lett. **8**(1), 31–35 (2008).
14. V. J. Sorger, R. F. Oulton, J. Yao, G. Bartal, and X. Zhang, "Plasmonic Fabry-Pérot nanocavity," Nano Lett. **9**(10), 3489–3493 (2009).
15. M. K. Seo, S. H. Kwon, H. S. Ee, and H. G. Park, "Full three-dimensional subwavelength high-Q surface-plasmon-polariton cavity," Nano Lett. **9**(12), 4078–4082 (2009).
16. J. R. Arias-González, and M. Nieto-Vesperinas, "Resonant near-field eigenmodes of nanocylinders on flat surfaces under both homogeneous and inhomogeneous lightwave excitation," J. Opt. Soc. Am. A **18**(3), 657 (2001).
17. D. Amarie, T. D. Onuta, R. A. Potyrailo, and B. Dragnea, "Submicrometer cavity surface plasmon sensors," J. Phys. Chem. B **109**(32), 15515–15519 (2005).

#138973 - $15.00 USD Received 30 Nov 2010; revised 27 Jan 2011; accepted 28 Jan 2011; published 14 Feb 2011

18. M. Bora, B. J. Fasenfest, E. M. Behymer, A. S.-P. Chang, H. T. Nguyen, J. A. Britten, C. C. Larson, J. W. Chan, R. R. Miles, and T. C. Bond, "Plasmon resonant cavities in vertical nanowire arrays," Nano Lett. **10**(8), 2832–2837 (2010).
19. C. G. Biris, and N. C. Panoiu, "Nonlinear pulsed excitation of high-Q optical modes of plasmonic nanocavities," Opt. Express **18**(16), 17165–17179 (2010), http://www.opticsinfobase.org/abstract.cfm?uri=oe-18-16-17165.
20. C. A. Pfeiffer, E. N. Economou, and K. L. Ngai, "Surface polaritons in circularly cylindrical interface: surface plasmons," Phys. Rev. B **10**(8), 3038–3051 (1974).
21. S. A. Maier, P. E. Barclay, T. J. Johnson, M. D. Friedman, and O. Painter, "Low-loss fiber accessible plasmon waveguide for planar energy guiding and sensing," Appl. Phys. Lett. **84**(20), 3990 (2004).
22. C. H. Dong, X. F. Ren, R. Yang, J. Y. Duan, J. G. Guan, G. C. Guo, and G. P. Guo, "Coupling of light from an optical fiber taper into silver nanowires," Appl. Phys. Lett. **95**(22), 221109 (2009).
23. P. Dawson, J. P. Goudonnet, and F. de. Fornel, "Imaging of surface plasmon propagation and edge interaction using a photon scanning tunneling microscope," Phys. Rev. Lett. **72**(18), 2927–2930 (1994).
24. M. Sumetsky, "Mode localization and the Q-factor of a cylindrical microresonator," Opt. Lett. **35**(14), 2385–2387 (2010).
25. B. Hecht, H. Bielefeldt, L. Novotny, Y. Inouye, and D. W. Pohl, "Local excitation, scattering, and interference of surface plasmons," Phys. Rev. Lett. **77**(9), 1889–1892 (1996).
26. A. Bouhelier, and G. P. Wiederrecht, "Surface plasmon rainbow jets," Opt. Lett. **30**(8), 884–886 (2005).
27. J. C. Knight, G. Cheung, F. Jacques, and T. A. Birks, "Phase-matched excitation of whispering-gallery-mode resonances by a fiber taper," Opt. Lett. **22**(15), 1129–1131 (1997).
28. V. A. Sychugov, V. P. Torchigin, and M. Y. Tsvetkov, "Whispering-gallery waves in optical fibres," Quantum Electron. **32**(8), 738–742 (2002).
29. E. D. Palik, *Handbook of Optical Constants of Solids* (Academic Press, New York, 1998).
30. A. W. Poon, R. K. Chang, and J. A. Lock, "Spiral morphology-dependent resonances in an optical fiber: effects of fiber tilt and focused Gaussian beam illumination," Opt. Lett. **23**(14), 1105–1107 (1998).

1. Introduction

Plasmonic resonators relying on resonance of surface plasmon polaritons (SPPs) in micro/nano metallic structures have been attracting extensive interests due to their potential of ultra-tight electromagnetic field confinement [1,2]. In the past years, a number of metallic SPP cavities, including microdisks [2–4], micropillars [5], microrings [6–9], Fabry-Pérot structures [10–15], spherical micro/nano particles [16–17] and nanowire arrays [18–19] have been reported, among which disk or closed-loop ring cavities, benefitted from their highly efficient recirculation of SPPs, offer opportunities to yield high quality (high-Q) plasmonic resonance [2, 8]. So far, high-Q plasmonic resonators are realized with strong confinement of SPPs in 3 dimensions, i.e., besides the circulation plane, the resonant modes are also well localized in the third direction (perpendicular to the circulation plane). Here we propose a metallic cylindrical cavity with strong confinement in only 2 dimensions, and experimentally observe high-Q plasmonic resonances of whispering gallery (WG) modes in an Au micro-cylinder.

2. Theoretical model

The cylindrical cavity proposed in this work is sketched in Fig. 1(a), a metallic cylinder with diameter of D and length L>>D, is employed for supporting plasmonic WG modes in the cross-section plane vertical to the axis of the cylinder. A fiber taper, perpendicularly coupled to the cylinder, is used for SPP excitation. For structural resemblance [20], a decoiled metallic film with an equivalent width of the cylinder circumference (πD), is illustrated in Fig. 1(b) to visualize the SPP excitation, propagation and interference on the surface of the cylinder. At the excitation point (x=0), guiding modes of the fiber taper evanescently couple into the SPP modes of the metallic cylinder when the phase-matching condition is fulfilled [21, 22]. Inheriting momentum of the excitation light from the fiber taper, the excited SPP modes propagate along the x direction and spread out at y-direction (the axis direction of the cylinder) [23]. When it propagates back to the excitation point after one circle with x=πD, a fraction of the SPP self-interferes and recirculates around the cylinder, resulting in a cylindrical plasmonic resonator. Despite of the leakage of the SPP along the axis direction, it is possible to obtain high-quality SPP resonance in such a 2-dimension confined metallic cylinder, as high-quality optical resonance in a 2-dimension confined dielectric cylinder has been theoretically predicted very recently [24].

#138973 - $15.00 USD Received 30 Nov 2010; revised 27 Jan 2011; accepted 28 Jan 2011; published 14 Feb 2011

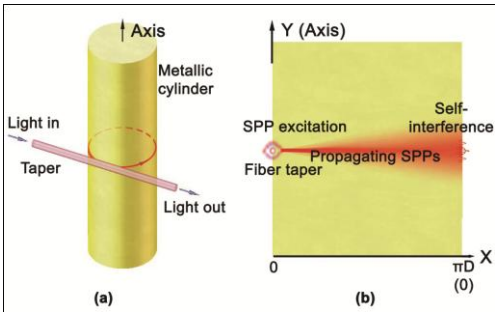

Fig. 1. Schematic illustration of plasmonic resonance of WG modes in a metallic cylinder cavity. (a) Metallic cylinder with a fiber taper for SPP excitation. (b) Structural resemblance of the decoiled metallic cylinder.

3. Experimental

Experimentally, the metallic cylinder used in this work is a piece of Au solder wire from a commercial laser diode chip (DL-3147-065, Sanyo), with diameters around 30 μm and excellent diameter uniformity. The fine surface quality of the cylinder is shown in the scanning electronic micrograph (Fig. 2(a)). To construct the resonator, we erected the Au wire in air, and used a biconical fiber taper with waist diameter of about 1 μm for SPP excitation. To excite SPP of the Au wire, we sent a broadband light (350 nm~1750 nm, Supeik Compact, Koheras) into the fiber taper, and gradually moved the taper toward the surface of the Au wire (D=29 μm), until obvious scattering occurred on the surface of the wire, as shown in Fig. 2(b). In the experiments, the coupling angle α (denotes the cross angle between the fiber taper and the Au wire), can be continuously adjusted for changing the excitation condition. The validity and mechanism of SPP excitation with the configuration shown in Fig. 2(b) has been verified in similar structures [2, 21]: the phase matching requirement between the guided mode of the fiber taper and the Au wire is fulfilled by scattering at the coupling area, and the propagating SPPs along the surface of the Au wire are excited by the in-plane component of incident wave vector of the guided light in the fiber taper. In Fig. 2(b), a red-color scattering light is clearly seen near the coupling area, indicates the efficient SPP excitation on the surface of the Au wire: the shorter-wavelength components of the SPP suffer higher loss than the longer-wavelength, resulting in higher fraction of long wavelength SPPs [25,26].

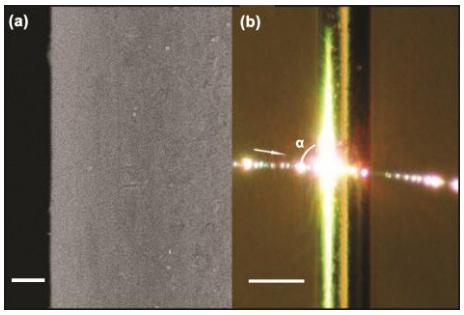

Fig. 2. Microscope images of a 29-μm-diameter Au wire. (a) Scanning electron microscope image of the wire surface. Scale bar, 2 μm. (b) Optical microscope image of the wire excited by a supercontinuum using a fiber taper. The direction of the excitation light is denoted by a white arrow, and the coupling angle (the cross angle between the fiber taper and the Au wire) is denoted as α. Scale bar, 30 μm.

4. Results and discussion

Typical SPP resonance spectra of a 25-μm-diamter Au wire, when excited by a fiber taper with waist diameter of 1 μm and coupling angle α of 90°, are given in Fig. 3(a), in which resonance feature is clearly seen. The spectra are normalized by the maximum intensity

#138973 - $15.00 USD Received 30 Nov 2010; revised 27 Jan 2011; accepted 28 Jan 2011; published 14 Feb 2011

excluding the sharp intensity peak. For better characterization, all the resonant dips in Fig. 3(a) are fitted by Lorentzian curves (red lines). In a cylindrical cavity [27], the SPP modes in the Au cylinder can be categorized as SPP_{lm}, where l is the plasmonic mode number and m is the azimuthal mode number [2]. Here, when the propagation constants of the SPP modes ($\overline{\beta}$) in the Au cylinder matches that of the excitation light in the fiber taper (β), that is [27–28]

$$\overline{\beta} = \beta = [k^2 n^2 - 2.405^2 / \rho^2]^{1/2}, \quad (1)$$

the SPP WG modes can be excited in the Au cylinder, in which n is the refractive index of the fiber taper, k is the wave vector of the light in the fiber taper, and ρ is the radius of the taper. Therefore, the azimuthal mode number m can be obtained by periodic boundary condition

$$L \cdot \overline{\beta} = 2\pi \cdot m, \quad (2)$$

where L is the single-circulation path of the SPP WG mode and is related to the free spectral range (FSR) of the SPP WG resonance by [8]

$$FSR = \lambda^2 \Big/ [L \cdot (n_{Au} - \lambda \frac{dn_{Au}}{d\lambda})], \quad (3)$$

in which n_{Au} is the refractive index of Au [29].

In the cylinder cavity studied here, the lower-order (i.e., the smaller value of l) plasmonic WG mode is tend to offer higher-quality resonance due to its lower divergence in the recirculation. For lowest order plasmonic mode (l=1),

$$L_{l=1} = \pi D, \quad (4)$$

and therefore m and FSR for the lowest mode (l=1) can be obtained. For example, around 1565-nm wavelength in Fig. 3(a), the calculated FSR of the SPP_{1m} modes of the Au wire (24.7 nm) agrees well with measured FSR (25.1 nm).

For higher order modes, e.g., l=2, the azimuthal mode number m can be obtained by using measured FSR incorporated with Eqs. (2) and (3).

By using the above-mentioned categorization, two classes of plasmonic modes (l=1, 2) are identified in Fig. 3(a), with measured FSRs of about 25.1 nm for SPP_{1m} modes and 25.4 nm for SPP_{2m} modes, respectively.

For further verification of the SPP resonance in these wires, we compared resonance spectra of the 25-μm-diameter wire with that of a 30-μm-diameter Au wire, as shown in Fig. 3(b). The upper spectra are truncated from Fig. 3(a), and the bottom ones are measured with the same fiber taper and coupling angle. The measured FSR of SPP_{1m} in the 30-μm-diameter Au wire around 1560 nm is 15.5 nm (16.8 nm in theory) and the ratio to the one of the 25-μm-diameter Au wire is approximately 0.62, which approaches the theoretical value (the ratio of the theoretical FSRs of the SPP_{1m}, 0.69).

The Q factors of the resonances in the Au wires were calculated by the Lorentzian-fitted curves (see Fig. 3(a)) in the range from 1554 nm to 1620 nm, with the highest figure of merit of 375 for $SPP_{1,78}$ in the 30-μm-diameter Au wire, as shown in Fig. 3(c). Although the Q factors obtained here is lower than those demonstrated in 3-dimensional-confined disk cavities [2, 3], much better SPP resonance is expected in metallic cylinders with much better surface qualities.

The statistic analysis of the Q factors of the resonance modes given in Fig. 3(c) shows that, the Q values of SPP_{1m} in the 30-μm-diameter Au wire (Q_{mean}=264) are averagely higher than the ones in the 25-μm-diameter (Q_{mean}=149), indicating higher Q factors can be obtained in thicker wires, similar to those observed in SPP disk cavities [2], in which larger disks usually yield higher Q factors.

#138973 - $15.00 USD Received 30 Nov 2010; revised 27 Jan 2011; accepted 28 Jan 2011; published 14 Feb 2011

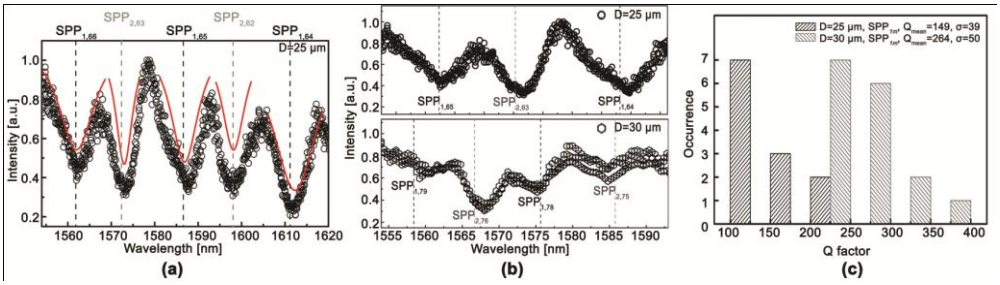

Fig. 3. Characterization of resonant WG modes in typical metallic cylinders. (a) Normalized transmission spectra of a 25-μm-diameter Au wire, with resonant dips fitted by Lorentzian curves (red lines). (b) Comparison of normalized transmission spectra of a 25- (upper) and a 30-μm-diameter (bottom) Au wires. The former is truncated from (a). (c) Statistical histograms of the measured Q factors of the first order SPP eigenmodes in the Au wires. Qmean represents the average Q value; σ is the standard deviation.

The plasmonic WG modes in the Au wire are also sensitive to the excitation angle. Figure 4, for example, gives normalized transmission spectra of a 29-μm-diamter Au wire with different coupling angles, and also the corresponding optical micrographs and relative angles between the wire and the tapered fiber. Within the spectral range 1510–1600 nm, two categories of modes, SPP_{1m} and SPP_{2m}, are presented and investigated here. At small coupling angle (Fig. 4(a), α=50°), the WG resonances of the two lowest-order SPP eigenmodes are relatively weak and broadened (compared with Fig. 4(b) and (c)). As the coupling angle increases to nearly perpendicular coupling circumstances (Fig. 4(b), α=80°; Fig. 4(c), α=110°), the more pronounced plasmonic resonances are clearly identified. When the coupling angle increases to far beyond the perpendicular coupling condition (Fig. 4(d), α=140°), the resonances become weak again and most of the first- and second-order SPP eigenmodes (e.g., $SPP_{1,78}$, $SPP_{1,76}$, $SPP_{1,75}$, $SPP_{2,76}$, $SPP_{2,74}$, and $SPP_{2,75}$) are absent. Similar to those observed in dielectric cylindrical cavities [30], here the α-dependent WG resonance is originated from the self-interference of the propagating SPPs, as illustrated in Fig. 4(e). The self-interference is mainly established by partially overlapping the newly excited SPP modes and the propagating SPPs after one-circle propagation around the coupling point. Under the perpendicular coupling condition, the intensity distribution of the propagating SPP is symmetric with respect to the circulation plane (the dotted line) perpendicular to the axis of the wire, leaving the intensity maximum overlapped with the coupling point, which results in strong self interference. When the coupling angle deviates from the perpendicular coupling condition, the intensity maximum shifts away from the coupling point, and the interference becomes weak.

#138973 - $15.00 USD Received 30 Nov 2010; revised 27 Jan 2011; accepted 28 Jan 2011; published 14 Feb 2011

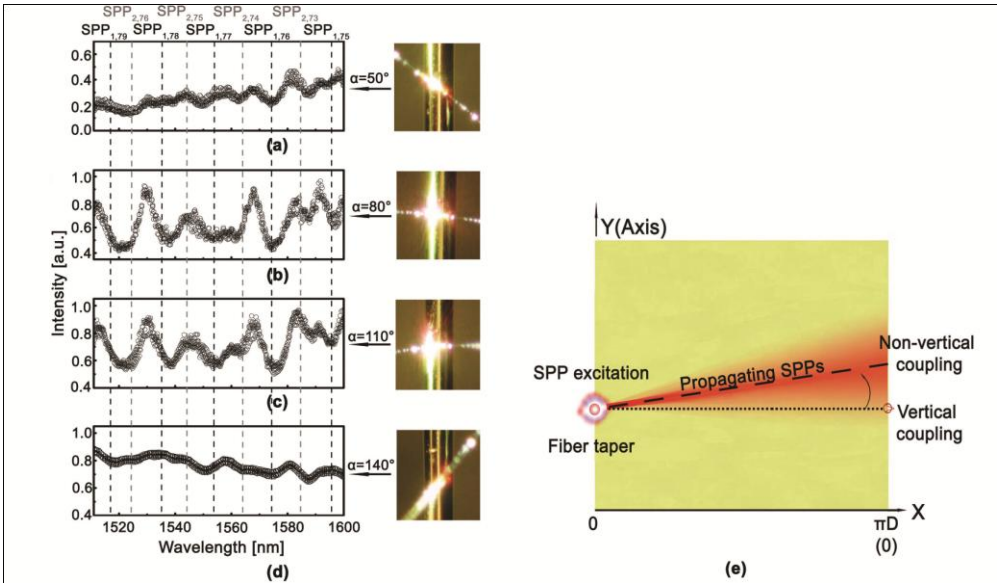

Fig. 4. Plasmonic WG resonance versus coupling angle α. The normalized transmission spectra are obtained from a 30-μm-diameter Au wire with α of (a) 50°, (b) 80°, (c) 110° and (d) 140°, separately. Optical images at the right column correspond to the recorded spectra with measured α. (e) Structural resemblance of the decoiled metallic cylinder under non-vertical coupling condition.

5. Conclusion

So far we have experimentally observed the WG resonances of SPPs on the surface of Au cylinders using fiber-taper-coupling technique. Although SPPs leak out along the axis direction, quality factors of the identified resonant SPP modes around a 30-μm-diameter Au cylinder go up to 375. The dependence of the resonance on the coupling angle verifies the self-interference model we employed for interpreting the resonance of propagating SPPs on the surface of the cylinder. Since the resonant SPP WG modes are obtained in simple metallic wires, results demonstrated in this work suggest possibilities to realize easy-fabrication, flexible, high-quality and compact SPP cavities for a variety of applications such as plasmonic sensing, as well as to extend the WG resonance model to diverse metallic structures such as metallic nanowires, nanotubes and nanopillars.

Acknowledgments

This work is supported by National Basic Research Program of China (No. 2007CB307003) and National Natural Science Foundation of China (Nos. 10974178 and 61036012).

#138973 - $15.00 USD Received 30 Nov 2010; revised 27 Jan 2011; accepted 28 Jan 2011; published 14 Feb 2011